# Integrated Geochemical Modeling of Magmatic Degassing and Hydrothermal Interaction at Kawah Ijen Volcano, Indonesia

Poster: V15p-206

N. Vigouroux (vigourouxcaillibotn@douglascollege.ca) - Dept. Earth and Environmental Sciences, Douglas College, New Westminster, BC, Canada
G. Williams-Jones - Physical Volcanology Group, Dept. Earth Sciences, Simon Fraser University, Burnaby, BC, Canada
K. Berlo - Dept. Earth and Planetary Sciences, McGill University, Montreal, QC, Canada
V. van Hinsberg - Dept. Earth and Planetary Sciences, McGill University, Montreal, QC, Canada
A.E. Williams-Jones - Dept. Earth and Planetary Sciences, McGill University, Montreal, QC, Canada

## Summary

Monitoring active volcanoes requires an understanding of degassing in relation to magma depth, temperature, composition, style of degassing and behavior of the hydrothermal system. We discuss subsurface degassing trends combined with measurements of fumarole gases and acid spring waters from the persistently degassing volcano, Kawah Ijen, Indonesia.

Compositions of matrix glass and melt inclusions representative of basaltic to trachytic magmas were determined. The behaviour of the volatile species ($D^{fluid\text{-}melt}$) during ascent, degassing and crystallisation was modeled for both open and closed system processes. Open system vapour fluxing dominates, as suggested by the large variations in the $H_2O$ and $CO_2$ contents of the melt inclusions. Modeled S $D^{fluid\text{-}melt}$ values suggest pressure (and dissolved $H_2O$ content), $fO_2$ and sulphide saturation play a role in controlling S release in the basaltic magma. As it evolves to trachyte, S partitioning into the fluid phase increases over two-fold. Halogen behaviour is strongly affected by apatite crystallisation.

From the glass data we model a best-fit gas composition and compare it to the fumarole gas compositions. The latter represent some of the most S- and $CO_2$-rich and Cl-poor vapours reported for arc volcanoes and are interpreted to reflect: 1) a major drop in S solubility as the basaltic magma evolves; 2) the inherently low halogen content due to apatite crystallisation; 3) condensation of the vapour upon ascent. Sulphur and C are concentrated in the vapour; Cl and F are lost to the liquid. The lack of S scrubbing implies that the gas C/S ratio is an important guide for magmatic activity.

## Background

Recent integrative studies of magmatic degassing have broadened our understanding of the link between subsurface exsolution of volatiles and surface gas emissions at active, open vent volcanoes (e.g., Aiuppa et al., 2010; Edmonds et al., 2010; de Moor et al., 2016). This study combines estimates of the magmatic fluid composition derived from melt inclusion data with measured surface fumarole and acid waters at Kawah Ijen volcano, Indonesia, in order to gain insight into possible modification/ scrubbing of magmatic gases by the hydrothermal system. A large hyper-acidic crater lake and acid stream runoff attests to the presence of this hydrothermal system. Any effects of the hydrothermal system on degassing are quantified by comparing the gas specie ratios in the modeled magmatic fluid with those measured in both the fumarole gases and the acidic waters.

Kawah Ijen and the Ijen Caldera Complex are located in eastern Java, Indonesia, along the volcanic front of the Sunda arc (Fig. 1a). Beneath Kawah Ijen, subduction of the 130 Ma Indo-Australian plate occurs at ~ 7 cm $yr^{-1}$, making it one of the fastest and oldest subducting plates (Syracuse and Abers, 2006). Water-rich fluid release from the subducting plate to the volcanic front is amongst the highest documented at arcs worldwide (Vigouroux et al., 2012) and results in volatile-rich magmas such as those found at Kawah Ijen.

Kawah Ijen is a small, active stratovolcano that sits on the eroded flank of the inactive Merapi volcano, at the intersection of the Ijen Caldera Complex rim and an intra-caldera lineament of small cinder cones and shields (Fig. 1b). The current configuration is a large (1 km wide) crater, ~ 300 m deep, partly filled with a hyper-acidic lake that drains into the Banyu Pahit river. The edifice is composed of basaltic to dacitic lavas and pyroclastic material and a vigorously degassing magmatic dome on the SE shore of the lake, whose surface is covered in native sulphur deposits.

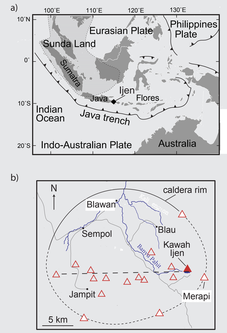


## Methodology

Samples of scoria from exposed layers of the edifice were collected in order to sample the most primitive and rapidly cooled material at Kawah Ijen, from which olivine phenocrysts and a few clinopyroxene crystals containing abundant glassy melt inclusions were hand picked (Vigouroux et al., 2012; Berlo et al., 2014). These data are compared to more felsic pyroclastic bombs sampled from the western crater rim, from which mostly orthopyroxene phenocrysts containing glassy melt inclusions were picked (Berlo et al., 2014). One sample of dome material containing a glassy interstitial melt globule (sample KV08-702; van Hinsberg et al., 2010b) is also compared. Glasses (including groundmass glass) were analyzed for major and minor elements, including S, Cl and F via EMPA, and $H_2O$ and $CO_2$contents were obtained via FTIR. In addition, the S Kα wavelength position for each melt inclusion was determined by detailed wavescan in order to estimate the $S^{2-}/S^{6+}$ ratio and the $fO_2$ of the melts. See Vigouroux et al. (2012) for details of the methodology. Olivine-hosted melt inclusion compositions were corrected for any post-entrapment modification (see Vigouroux et al., 2012), whereas the pyroxene inclusions were not. Therefore some of the variation in the compositions of these melt inclusions is likely to result from post entrapment crystallization, but this is expected to be small, particularly for elements incompatible in pyroxene.

Fumaroles on the active dome were sampled in 2007 and 2008 following the method of Giggenbach (1975). The sampling points were located on the top of the dome directly into the natural fumaroles and not from the exit of the pipes at the base of the dome, used by miners to cool and liquify the emanating sulfur gas. The selected vents represent well-established, high temperature (>350 °C) vents with high visible flow and without encrustations or mineral precipitates at the vent. See Berlo et al. (2014) and van Hinsberg et al. (2015) for details of the sampling and analytical procedures.

## Melt compositions

Olivine hosts have compositions of $Fo_{78\text{-}81}$ (Fo = forsterite %) and some contain inclusions of a Cr-rich oxide and rare inclusions of sulfide blebs (Berlo et al., 2014). Fig. 2 shows that olivine-hosted melt inclusions are basaltic in composition and classify as medium-K calc-alkaline magmas, as is typical of arc magmas in eastern Java and Bali (Vigouroux et al., 2012). The orthopyroxene-hosted melt inclusions are more evolved and have a total alkali content that places them near the border of the dacite and trachyte classifications. The glass globule from the dome material is rhyolitic in composition. Fig. 3 shows that $K_2O$ behaves as an incompatibleelement throughout the evolutionary sequence.

Fig. 4 summarizes the $H_2O$ and $CO_2$ contents recored in the melt inclusions and groundmass glasses and Fig. 5 shows the variation in volatile/$K_2O$ content of the melts as a function of pressure (calculated from the $H_2O$ and $CO_2$ partial pressures).




Fig. 5: Variation in the ratio of a) $H_2O$, b) S, c) Cl and d) F over $K_2O$ contents as a function of melt inclusion trapping pressure and depth. Basaltic matrix glass and dome rhyolitic glass samples have not been analysed for $H_2O$ and $CO_2$, therefore an arbitrary pressure of 0.1 MPa has been assigned to them for graphing purposes only. Insets in b) and d) show a zoom-in of the trachytic and rhyolitic samples.

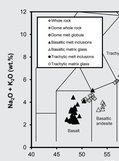


Fig. 2: Total alkalis versus $SiO_2$ (normalized on an anhydrous basis). Dome rhyolite glass represents interstitial melt within the dome rock. The basaltic melt inclusions are olivine-hosted. Basaltic matrix glass are from tephra. Trachytic melt inclusions are orthopyroxene-hosted and the corresponding matrix glasses are from pumice bombs. Whole rock data is from van Hinsberg et al. (2010b). Classification scheme from LeMaitre (2002).

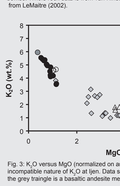


Fig. 3: $K_2O$ versus MgO (normalized on an anhydrous basis) showing the incompatible nature of $K_2O$ at Ijen. Data sources are the same as in Fig. 2 except the grey triangle is a basaltic andesite melt inclusion hosted in clinopyroxene.

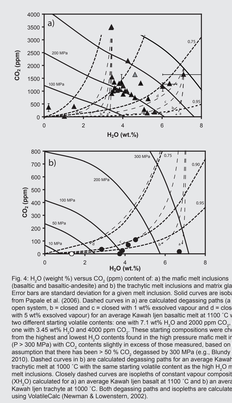


Fig. 4: $H_2O$ (weight %) versus $CO_2$ (ppm) content of: a) the mafic melt inclusions (basaltic and basaltic-andesite) and b) the trachytic melt inclusions and matrix glasses. Error bars are standard deviation for a given melt inclusion. Solid curves are isobars from Papale et al. (2006). Dashed curves in a) are calculated degassing paths (a = open system, b = closed and c = closed with 1 wt% exsolved vapour) for an average Kawah Ijen basaltic melt at 1100 °C with two different starting volatile contents: one with 7.1 wt% $H_2O$ and 2000 ppm $CO_2$, and one with 3.45 wt% $H_2O$ and 4000 ppm $CO_2$. These starting compositions were chosen from the highest and lowest $H_2O$ contents found in the high pressure mafic melt inclusions (P > 300 MPa) with $CO_2$ contents slightly in excess of those measured, based on the assumption that there has been > 50 % $CO_2$ degassed by 300 MPa (e.g., Blundy et al., 2010). Dashed curves in b) are calculated degassing paths for an average Kawah Ijen trachytic melt at 1000 °C with the same starting volatile content as the high $H_2O$ mafic melt inclusions. Closely dashed curves are isopleths of constant vapour composition ($XH_2O$ calculated for a) an average Kawah Ijen basalt at 1100 °C and b) an average Kawah Ijen trachyte at 1000 °C. Both degassing paths and isopleths are calculated using VolatileCalc (Newman & Lowenstern, 2002).

## Degassing models

**Behaviour of S:** As the melt evolves from basalt to trachyte, the solubility of S decreases (Fig. 5b), mainly associated with an increase in melt polymerization, fractionation of $Fe^{2+}$-bearing phases (Fe-oxides) and a drop in temperature (Masotta et al., 2016). In addition, as pressure drops and $H_2O$ degasses, oxygen fugacity decreases as well (Fig. 6b; Moussallam et al., 2014), further reducing the overall solubility of S in the melt (Zajacz, 2015), favoring instead the formation of a sulfide liquid or partitioning of S to the fluid phase (Fortin et al., 2015). Although $fO_2$ values for the Ijen basalts appear to lie below the threshold for sulphide saturation (based on SCSS calculations shown in Fig. 6a), there is evidence from the coupled behaviour of S and chalcophile elements in the melt inclusions that the melt may be sulphide saturated at depths > 200 MPa (Berlo et al., 2014). One possibility is that $CO_2$ fluxing, which draws $H_2O$ out of the melt, may have played a role in shifting the SCSS limit of the Ijen basalts to lower values, enabling sulfide saturation at high pressures (lower pressures increase the SCSS limit). The breakdown of an accumulated sulphide phase would release S to the melt or fluid phase, and if sulphide breakdown was promoted by magma mixing or differentiation, this would increase the fraction of S released to the fluid (DS fluid/melt increases as melt polymerization increases). There are too many unknowns to quantify the contribution of a sulphide liquid phase to the total S gas budget but we qualitatively show the effect of such a contribution in Fig. 11 (see discussion below).

**Behaviour of Cl and F:** The presence of apatite as mineral inclusions and in the matrix of the more evolved samples, combined with the co-variation of melt $P_2O_5$, Cl and F contents (Fig. 7) suggests that apatite controls the Cl and F content of the melt phase. The $P_2O_5$/Cl ratio of the basaltic samples is lower than would be expected from the crystallization of either Cl-apatite or F-apatite due to overprinting by F degassing (decreasing $K_2O$/ $P_2O_5$; Fig. 7c). In the more evolved samples, the fractionation of Cl-apatite is replaced by F-apatite and $K_2O$/Cl ratios become nearly constant as neither Cl degasses or is taken up by apatite. Only the trachytic matrix glass shows evidence of degassing. The $K_2O$/F ratio of the evolved melt is more variable and indicates a combination of uptake by F-apatite and degassing of F (Fig. 7c).

**Modelling:** Following the method described in Johnson et al. (2010), we model the evolution of the gas phase as magma ascends, cools and evolves chemically by combining information on the variation of S, Cl and F contents with $H_2O$ and $K_2O$ contents (Fig. 5) with equations of mass balance. After establishing the initial (undegassed) magmatic compositions, the volatile element partition coefficients between the melt and vapour fraction ($D^{vap\text{-}melt}$) are calculated for each melt inclusion (see Vigouroux, 2011 for details). Mass balance constraints are used to model: 1) open system degassing (Rayleigh fractionation); 2) closed system degassing (batch processes); and 3) open system vapour fluxing where the melt is re-equilibrated with a fluid phase introduced into the system from depth. Based on $H_2O$-$CO_2$ systematics (Fig. 4), the vapour fluxing models are most appropriate (Fig. 8 & 9).

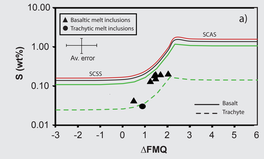


Fig. 6: a) Sulphur contents in the basaltic and trachytic melt inclusions (log scale) versus oxygen fugacity (represented as log units relative to the Fayalite-Magnetite-Quartz buffer, FMQ), calculated from the S Kα peak positions and converted to oxygen fugacity at a temperature of 1100 °C and 1000 °C for the basaltic and trachytic melt inclusions, respectively (see Vigouroux, 2011). Also shown are sulphur contents at sulphide-saturation (SCSS) for an average Kawah Ijen basalt at 1100 °C, calculated using the method of Fortin et al. (2015), at different pressures and corresponding $H_2O$ contents for an average Kawah Ijen basalt in equilibrium with a vapour phase composition of $XH_2O = 0.75$). The transition from sulphide- to sulphate-saturation and the critical $fO_2$ value are from Jugo (2009). Experimental data from dry basalt at 1300 °C and 1 GPa (Jugo et al., 2005a) is used to derive the absolute value of change in S solubility from sulphide- to sulphate-saturated conditions, a value which is then applied to the SCSS calculated for Kawahijen basalt in order to derive the sulphur content at anhydrite- (sulphate-) saturation (SCAS). In panel b) melt inclusion calculated trapping pressure ($P_{trap}$ - $P_{H2O}$) is plotted versus calculated $fO_2$.

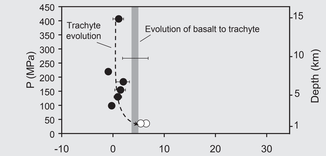


Fig. 9: Pressure (and depth) versus modeled $D^{fluid\text{-}melt}$ values for Cl within the trachytic magma and for a system where basaltic magma is evolving to trachytic compositions (see Vigouroux, 2011 for details of the modelling procedure). Model values are for vapour fluxing conditions (average between 1 and 5 wt% vapour) and open system degassing for the melt inclusions and trachytic matrix glasses, respectively. Error bars represent the standard deviation between the model results for 1 and 5 wt% vapour fluxing. Dashed curve highlights the trend within the trachytic melt inclusion data.

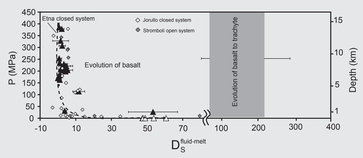


Fig. 8: Pressure (and depth) versus modeled $D^{fluid\text{-}melt}$ values for S within the Kawah Ijen basaltic magma and for the evolution of basaltic to trachytic compositions (see Vigouroux, 2011 for details of the modeling procedure). Model values are for vapour fluxing conditions (average between 1 and 5 wt% vapour) and open system degassing for the melt inclusions and basaltic matrix glasses, respectively. Error bars represent the standard deviation between the model results for 1 and 5 wt% vapour fluxing. Shown for comparison are S $D^{fluid\text{-}melt}$ values for the basaltic melt inclusions of Jorullo volcano, Mexico, under closed system degassing constraints (Johnson et al., 2010) and Stromboli volcano, Italy, under open system degassing constraints (Scaillet and Pichavant, 2005). The dashed curve represents the best-fit through $D^{fluid\text{-}melt}$ values obtained for Etna volcano, Italy (Spilliaert et al., 2006), under closed system degassing constraints.

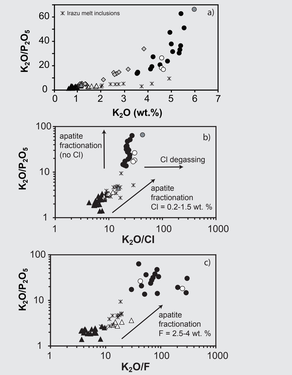


Fig. 7: Variation of the $K_2O/P_2O_5$ ratio with a) $K_2O$ content (wt%), b) $K_2O$/Cl ratio and c) $K_2O$/F ratio. Melt inclusions from Irazu volcano, Costa Rica (Benjamin et al., 2007; Sadofsky et al., 2008) are shown for comparison. Irazu has erupted lavas and pyroclastic material containing apatite phenocrysts. Combined with apatite compositions from mafic magmas near Colima volcano, Mexico (0.18 wt% Cl, 2.86-3.02 wt% F; Luhr and Carmichael, 1981), the Irazu apatite compositions (0.54-1.5 wt% Cl, 2.5-4 wt% F; Boyce and Hervig, 2009) define the $P_2O_5$/Cl and $P_2O_5$/F ratios of a liquid fractionating apatite.

## Gas compositions

As with most arc magmas, $H_2O$ is the dominant gas specie followed by $CO_2$ > $S_{total}$ ($SO_2$+$H_2S$) > $N_2$ > HCl > HF > minor species. The 2008 samples have $H_2$-$N_2$-Ar contents that reflect variable degrees of air contamination, whereas the 2007 samples are contaminated by air-saturated groundwater (Fig. 10). Compared to other arc volcanoes, Kawah Ijen gases (2008) have low $H_2O$/$S_{total}$ and $CO_2$/$S_{total}$ weight ratios as well as low $H_2O$/$CO_2$ (Fig. 11). The 2008 gases also plot at the high end of $S_{total}$ /HCl and $S_{total}$/HF weight ratios compared to other arc volcanoes (Fig. 12).

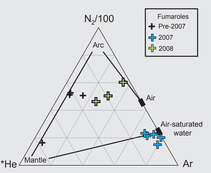


Fig. 10: $He$-$N_2$-$Ar$ ternary diagram (on a molar basis) comparing the Kawah Ijen fumarole gases with air and air-saturated water (e.g., Giggenbach, 1987). "Arc-type" gases are enriched in $N_2$ and "Mantle-type" gases are enriched in He (Giggenbach and Matsuo, 1991). Pre-2007 data is compiledfrom Delmelle et al. (2000).

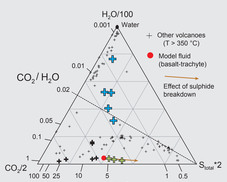


Fig. 11: $H_2O$-$CO_2$-$S_{total}$ ternary diagram (on a weight basis) comparing Kawah Ijen with high temperature (> 350 °C) fumarole gases from other arc volcanoes (see Vigouroux, 2011 for data sources). The dashed line, at a $CO_2/H_2O$ weight ratio of 0.02, represents a lower limit of realistic magmatic vapour compositions at arc volcanoes (equivalent to a vapour $XH_2O$ of 0.99). Vapour compositions that lie above this line are at risk of containing a meteoric water component. Also shown is the best-fit model magmatic fluid composition derived from the melt inclusion data (see previous section for details) and the orange arrow illustrates the hypothetical effect of sulphide breakdown as the basaltic magma evolves.

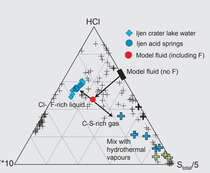


Fig. 12: HF-HCl-$S_{total}$ ternary diagram (on a weight basis) comparing Kawah Ijen with high temperature (> 350 °C) fumarole gases from other arc volcanoes. Also shown are crater lake and acid spring waters from Kawah Ijen (Delmelle et al., 2000; Palmer, 2009) and the best-fit model magmatic fluid composition (S-Cl only) derived from the melt inclusion data (see previous section for details). The original magmatic fluid (including F) is inferred from the intersection of the linear series relating the acidic waters and the fumarole gases with the line relating the model fluid composition and the F apex.

## Comparison with model results

Assuming the $H_2O$/$CO_2$ ratio of the 2008 gases have been minimally impacted by the hydro-thermal system (Fig. 10) and are representative of the gases being emitted by the magmatic system at Ijen, then our model gas composition has a $XH_2O$ = 0.9. As such, the $XSO_{2\ (total)}$ of the fluid is 0.017 and the XHCl is 0.005, assuming a differentiating magma body (basalt-trachyte). This modelled fluid composition is in good agreement with the 2008 fumarole compositions in $H_2O$-$CO_2$-$S_{(total)}$ space (Fig. 11). In HCl-HF-$S_{(total)}$ space, a line linking the acid waters and the 2008 gases can be interpreted as both a mixing line (when boiling of acid waters is mixed with magmatic vapours as in 2007) and an unmixing line (when condensation of the magmatic fluid results in a Cl- and F-enriched liquid and a S-enriched vapour). The extension of a line from the S/Cl ratio of the model magmatic fluid to the F apex will intersect the mixing/unmixing line at a point which represents our best estimate of the original magmatic fluid S-Cl-F composition (Fig. 12).

## References

Aiuppa, A., Bertagnini, A., Metrich, N., Moretti, R., Di Muro, A., Liuzzo, M., Tamburello, G., 2010. A model of degassing for Stromboli volcano. Earth Planet. Sci. Lett. 295 (1-2), 195-204.
Benjamin, E.R., Plank, T., Wade, J.A., Kelley, K.A., Hauri, E.H., Alvarado, G.E., 2007. High water contents in basaltic magmas from Irazú volcano, Costa Rica. J. Volcanol. Geotherm. Res. 168 (1-4), 68-92.
Berlo, K., van Hinsberg, V.J., Vigouroux, N., Gagnon, J.E., Williams-Jones, A.E., 2014. Sulfide breakdown controls metal signature in volcanic gas at Kawah Ijen volcano, Indonesia. Chem. Geol. 377, 119-127.
Blundy, J., Cashman, K., Rust, A., Witham, F., 2010. A case for CO2-rich arc magmas. Earth Planet. Sci. Lett. 290 (3-4), 289-301.
Boyce, J.W., Hervig, R.L., 2009. Apatite as a monitor of endogenic processes on Io: Evidence from the Culann region. Icarus 200 (1), 109-145.
de Moor, J.M., Aiuppa, A., Avard, G., Wehrmann, H., Dunbar, N., Muller, C., Tamburello, G., Giudice, G., Liuzzo, M., Conde, V., Galle, B., 2016. Turmoil at Turrialba Volcano (Costa Rica): Degassing and eruptive processes inferred from high-frequency gas monitoring. JGR Solid Earth. 121 (8), 5761-5775.
Delmelle, P., Bernard, A., Kusakabe, M., Fischer, T. P., Takano, B., 2000. Geochemistry of the magmatic-hydrothermal system of Kawah Ijen volcano, East Java, Indonesia. J. Volcanol. Geotherm. Res. 97 (1-4), 31-53.
Edmonds, M., Aiuppa, A., Humphreys, M., Moretti, R., Giudice, G., Martin, R. S., Herd, R.A., Christopher, T., 2010. Excess volatiles supplied by mingling of mafic magma at an andesite arc volcano. Geochem. Geophys. Geosyst. 11 (4), Q04005.
Fortin, M.-A., Riddle, J., Desjardins-Langlais, Y., Baker, D.R., 2015. The effect of water on the sulfur concentration at sulfide saturation (SCSS) in natural melts. Geochim. Cosmochim. Acta. 160, 100-116.
Giggenbach, W. F., 1975. A simple method for the collection and analysis of volcanic gas samples. Bull. Volcanol. 39 (1), 132-145.
Giggenbach, W. F., 1987. Redox processes governing the chemistry of fumarolic gas discharges from White Island, New Zealand. Applied Geochemistry, v. 2, p. 143-161.
Jugo, P. J., 2009. Sulfur content at sulfide saturation in oxidized magmas. Geology 37 (5), 415-418. Publication Info: Geology, Geological Society of America, Boulder, CO, United States. Publication Info: Applied Geochemistry, Applied Geochemists Group, Edinburgh, Scotland, United Kingdom.
Jugo, P. J., 2009. Sulfur content at sulfide saturation in oxidized magmas. Geology 37 (5), 415-418.
Jugo, P. J., 2009. Sulfur content at sulfide saturation in oxidized magmas. Geology 37 (5), 415-418.
Jugo, P. J., Luth, R. W., Richards, J. P., 2005. An experimental study of the sulfur content in basaltic melts saturated with immiscible sulfide or sulfate liquids at 1300 °C and 1.0 GPa. J. Petrol. 46 (4), 783-798.
La Marche, R.W. (Ed.), 2002. Igneous Rocks: A Classification and Glossary of Terms, 2nd ed. Cambridge University Press, Cambridge, U.K.
Luhr, J. F., Carmichael, I. S. E., 1981. The Colima volcanic complex, Mexico Part I. Late-quaternary cinder cones. Contrib. Mineral. Petrol. 76 (1), 127-147.
Masotta, M., Pontesilli, A., Mollo, S., Armienti, P., Ubide, T., Nazzari, M., Scarlato, P., 2016. Clinopyroxene-liquid thermometers and barometers specific to alkaline differentiated magmas. Contrib. Mineral. Petrol. Geochem. Cosmochem. Acta. 178, 26-43.
Moussallam, Y., Edmonds, M., Scaillet, B., Peters, N., Gennaro, E., Sides, I., Oppenheimer, C., 2016. The impact of degassing on the oxidation state of basaltic magmas: A case study of Kilauea volcano. EPSL. 450, 317-325.
Newman, S., Lowenstern, J.B., 2002. VolatileCalc: A silicate melt-H2O-CO2 solution model written in Visual Basic for excel. Comput. Geosci. 28, 597-604.
Palmer, M. R., 2009. Boron isotope systematics of Kawah Ijen volcanic system, East Java, Indonesia. Chem. Geol. 267 (3-4), 228-235. Publication Info: Chemical Geology, Elsevier, Amsterdam, Netherlands.
Papale, P., Moretti, R., Barbato, D., 2006. The compositional dependence of the saturation surface of H2O-CO2 fluids in silicate melts. Chem. Geol. 229 (1-3), 78-95.
Sadofsky, S.J., Portnyagin, M., Hoernle, K., van den Bogaard, P., 2008. Subduction cycling of volatiles and trace elements through the Central American volcanic arc: evidence from melt inclusions. Contrib. Mineral. Petrol. 155 (4), 433-456.
Scaillet, B., Pichavant, M., 2005. A model for sulphur degassing during explosive volcanic eruptions. Geochem. Geophys. Geosyst. 6 (4), Q04007.
Spilliaert, N., Allard, P., Metrich, N., Sobolev, A.V., 2006. Melt inclusion record of the conditions of ascent, degassing, and extrusion of volatile-rich alkali basalt during the powerful 2002 flank eruption of Etna volcano (Italy). J. Geophys. Res. Solid Earth. 111 (B4), B04203.
Syracuse, E. M., Abers, G. A., 2006. Global compilation of variations in slab depth beneath arc volcanoes and implications. Geochem. Geophys. Geosyst. 7 (5), Q05017.
van Hinsberg, V., Berlo, K., Sumarti, S., van Bergen, M., Williams-Jones, A.E., 2010b. Extreme alteration by hyperacidic brines at Kawah Ijen volcano, East Java, Indonesia: 2. Fluid-mineral isotopic and element fluxes. J. Volcanol. Geotherm. Res. 196 (3-4), 169-184.
van Hinsberg, V., Vigouroux, N., Palmer, S., Berlo, K., Mauri, G., Williams-Jones, A.E., McKenzie, J., Williams-Jones, G., Fischer, T., 2015. Element flux to the environment of the passively degassing crater lake hosting Kawah Ijen volcano, Indonesia, and implications for estimates of the global volcanic flux. Geol. Soc. London, Spec. Pub., 437 (1), 9.
Vigouroux, N., 2011. Volatile Behaviour in Basaltic to Trachytic Magmas: Insights from Melt Inclusions and Fumarole Gases at Kawah Ijen Volcano, Indonesia. Ph.D. Thesis, McGill University, Montreal, QC, Canada, 1-300.
Vigouroux, N., Wallace, P.J., Williams-Jones, G., Kelley, K., Berlo, K.A., Williams-Jones, A.E., 2012. The sources of volatile and fluid-mobile elements in the Sunda arc: A melt inclusion study from Kawah Ijen and Tambora volcanoes. Volcanotectonic Geochem. Geophys. Geosyst. 13 (9), doi.org/10.1029/2012GC004192
Zajacz, Z., 2015. The effect of melt composition on the partitioning of oxidized sulfur between silicate melts and magmatic volatiles. Geochim. Cosmochim. Acta. 158, 223-244.

## Acknowledgments

The authors would like to thank the Kawah Ijen Park service and particularly Tom Mulja and Niken Widyastuti of East Asia Minerals for their help. The Kawah Ijen research team, namely Guillaume Mauri, Stephanie Palmer, Samantha Scher, as well numerous other volunteers, offered valuable help in the field. Local miners Pa Im and Jumanto were invaluable for their assistance in the field, especially with dome fumarole sampling. We acknowledge Tobias Fischer (University of New Mexico) for analysis of the fumarole gas samples, as well as John Donovan (University of Oregon) and Lang Shi (McGill University) for assistance with the microprobe analyses. Funding for this work was provided by an NSERC-CRD grant to A.E. Williams-Jones and G. Williams-Jones.